Polymer 50 (2009) 547–552

Contents lists available at ScienceDirect

Polymer

journal homepage: www.elsevier.com/locate/polymer

Control on the topological structure of polyolefin elastomer by reactive processing

Jianye Liu, Wei Yu*, Wei Zhou, Chixing Zhou

Advanced Rheology Institute, Department of Polymer Science and Engineering, Shanghai Jiao Tong University, Shanghai 200240, PR China

ARTICLE INFO

Article history:
Received 8 October 2008
Received in revised form
6 November 2008
Accepted 14 November 2008
Available online 28 November 2008

Keywords:
Complex flow field
Control on topology
Degradation

ABSTRACT

The feasibility of preliminary tailoring of the long chain branched (LCB) polymer through complex flow field was evaluated in the torque rheometer, for the reaction of melt polyolefin elastomer (POE) with peroxides at elevated temperatures. With the compensation of temperature, the strength of complex shear flow could be the only factor affecting the reaction kinetics and mechanism. The results of sample characterization by the rheological and dilute polymer solution methods indicated that the degradation mainly made the length of LCB arm shorter and shorter as the rotational speed increases. Extremely, a certain amount of LCB degraded to be linear chains again due to the scission approaching the branching point at intense mixing condition. One new LCB index (D_{LCB}) was defined from nonlinear oscillatory shear, and a nearly linear relationship between it and long chain branching index (LCBI) was found, which can be a map to quantify LCB level by Fourier Transform Rheology (FTR).

1. Introduction

Since long chain branched (LCB) polymer is always desirable for many applications such as foaming and film blowing, how to attain polymeric materials with appropriate topological structure and suitable content of LCB is crucial. Optimal tailoring of these LCB properties has become a major goal firstly in the polyolefin industry. Such kind of tailoring may now be possible during the polymerization of polyolefin due to the development of metallocene catalysts [1], but only resulting in a very small amount of LCB. It would be furthermore significant if such tailoring can be realized through the highly efficient post-polymer processing. Reactive processing of polyolefin in melt state often takes use of chemical modifications, such as free radical courses, where two dominating reactions happen. Coupling between two macroradicals brings on LCB or gels and increases the molecular weight, while scission makes the molecular weight decrease. No matter what kind of reactions dominate, the final product of reactive processing of polyolefin is usually a mixture of linear molecules and branched ones with certain degree of branching and some kind of random topological structure.

Generally, coupling of two macromolecular radicals is not easy to control since it is a kind of irreversible conversion. Although it has been shown that flow field will affect the formation of LCB in polyethylene [2], it is impossible to control the molecular structure and LCB's content only by coupling reaction at present. On the other hand, chain scission can be regarded as a reversible reaction, depending on the recombination rate and the speed of the fractured chain moving out of the capture radius, which is very sensitive to the imposed shear flow field. For example, we found that nonlinear shear flow favored effective chain scission for melt polyolefin elastomer (POE) [3]. Moreover, in simple shear flow, it is confirmed through Fourier Transform Rheology (FTR) that the degradation of melt POE starts on the created LCB and the extent of LCB decreases with the shear rate [4]. The substantial factor inducing these phenomena is the long relaxation time of the created LCB compared with the original linear chain. There seems to be a kind of selectivity of shear rate on the polymer chain for degradation, which hints a possibility to control and design the molecular structure of polymer chains during reactive processing.

In the present paper, we will show the way to control the reaction and the microstructure of melt POE during processing in the torque rheometer at elevated temperatures. Products with different structures were obtained by different processing conditions with the same formula. All the products were fully characterized through the methods of rheology, including creep, linear and nonlinear oscillation shear followed by FTR [4–9]. Besides, dynamic light scattering (DLS) and the intrinsic viscosity [η] of dilute polymer solution were also utilized to characterize the products created in different processing conditions. This work serves as the preliminary trials to design, characterize and control the molecular structures during reactive polymer processing.

2. Experimental

2.1. Materials

The experimental polymer used in this study is poly(ethylene-*co*-α-butene) (PEB). It was produced by copolymerization of

* Corresponding author. Tel.: +86 21 54743275; fax: +86 21 54741297.
E-mail address: wyu@sjtu.edu.cn (W. Yu).

0032-3861/$ – see front matter © 2008 Elsevier Ltd. All rights reserved.
doi:10.1016/j.polymer.2008.11.030

Table 1
The processing conditions and the characteristic data for each sample.

Sample code	RSC10	RSC20	RSC40	RSC60	RSC100	PEB
Rotational speed (rpm)	10	20	40	60	100	–
Set value of temperature (°C)	160	157	154	148	136	–
Duration[a] (min)	15	25	25	25	25	25
η_0 (kPa s)	388	243	149	59.9	30.4	7
$[\eta]$ (dL g^{-1})	1.36	1.33	1.29	1.20	1.10	0.88
$\overline{R}_h$ (nm)	266.4	232.5	92.5	34.9	19.2	5.6
A	0.181	0.146	0.122	0.073	0.049	0.028
D_{LCB}/a_I	0.241/5.21	0.199/4.35	0.184/3.68	0.109/2.35	0.0542/1.66	0/1
LCBI	0.452	0.347	0.262	0.126	0.075	0

[a] The onset of the processing duration is appropriately considered as the point when the polymer melts completely.

ethylene with α-butene via a single-site metallocene catalyst technique resulting in the ethyl short branches. PEB grade Tafmer A-4085, with the butene content of 13.3 mol% (determined from ^{1}H NMR analysis), melt flow index of 3.6 g/10 min (190 °C, 2.16 kg), and density of 0.885 g cm^{-3} (20 °C), was obtained from Mitsui Chemicals, Japan. Its number average molecular weight (M_n) and molecular weight distribution (M_w/M_n) are 55.4 kg mol^{-1} and 2.3, respectively. Dicumyl peroxides (DCPs, chemical pure), purchased from Shanghai Chemicals Factory, PR China, were used without any further treatment. The decomposition rate constant of DCP, k_d, is 9.233×10^{-7} s^{-1} at 90 °C and 3.40×10^{-3} s^{-1} at 160 °C, as provided by the supplier, and the half-life time is 208.5 h and 204 s at 90 °C and 160 °C, correspondingly.

2.2. Sample preparation and reaction processing

The pellets of PEB (45 g) were impregnated with an acetone solution of DCP (0.1 g) over 12 h at room temperature, which was followed by evaporation at a low pressure to remove the residual solvent. Then the PEB sample with DCP concentration of 8.23×10^{-3} mol kg^{-1} was premixed in a torque rheometer (Haake Polylab OS system, Thermo Fisher, Germany) at 90 °C with the rotor speed 60 rpm and taken out after 6 min to make into small pieces. Even though the half-life time of DCP at 90 °C is as long as 208.5 h, it is still possible to have a small amount of decomposition during the preparation. However, such small amount of reaction will not affect our experimental results.

The pieces of well-premixed samples were then put into the torque rheometer again to carry out the reaction processing at elevated temperatures. The detailed processing conditions and the codes for all samples are listed in Table 1, as well as the torque and temperature curves are shown in Fig. 1. The numbers in the name of the samples denote the rotational speed of rotors during mixing. When the processing terminated, 0.5 wt% Irganox 1010 (Ciba, Switzerland) was added into each product as the antioxidants followed by extra 3 min mixing, in order to stabilize the products during the subsequent rheological measurements.

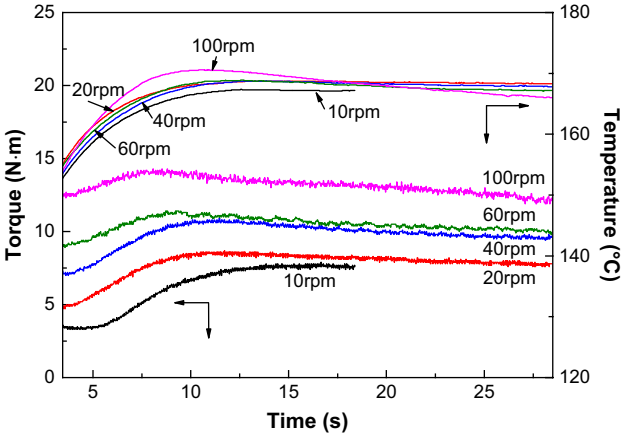

Fig. 1. Torque and temperature evolutions for all RSC reaction courses.

2.3. Rheological measurement

The rheological tests were all performed on a rotational rheometer (Gemini 200HR, Bohlin Instruments, UK) with parallel plate geometry of 25 mm in diameter and a gap of 1 mm, after the samples were compressed into sheet (thickness ≈ 1 mm) at 90 °C under 12 MPa. The stability of the sample was checked through the measurement of G' and G'' at 0.1 Hz in the linear viscoelastic region. Little changes in dynamic modulus had been found (0.9% for G' and 1.3% for G'') over a long period (200 min) at 160 °C with a strain amplitude of 5%, which illustrated that DCP has been consumed completely during mixing and the effect of the thermal oxidation can be excluded.

The measurements of small amplitude oscillatory shear (SAOS) were carried out for all products. The strain amplitude sweeps were applied, and the corresponding critical strain amplitudes are 24.6% and 18.9% for the original PEB and RSC10 at the same frequency. Frequency sweeps were performed in the range of 0.01–100 rad s^{-1} with a given strain amplitude of 5%. Afterwards the nonlinear oscillatory shear experiments were performed for each product at 0.1 Hz. The data of torque wave were recorded after the sample achieved the steady state with the certain strain amplitude. There were 16,384 raw torque data points acquired every four sampling periods and a signal-to-noise ratio at least 1000:1 in the spectrum of every single measurement is reached in such type of experiment. The zero viscosity of each sample was tested by creep experiment with the constant stress of 5 Pa, which was within the linear viscoelastic region.

2.4. Purification and characterization in dilute polymer solution

All the products were taken out of the torque rheometer for further measurements of rheology and DLS. There was no insoluble fraction left for each sample after employing Soxhlet extraction cycle for 24 h with xylene as the solvent at 120 °C, which indicated that no gels were created in all the products. Then each sample was fully dissolved in xylene and added slowly into acetone, which was followed by filtration. The resulting peroxide-modified POE was washed with acetone three times before drying in a vacuum oven at 50 °C for 48 h.

The hydrodynamic radius and its distribution of all samples were determined in the dilute polymer toluene solution at 70 °C by the experiments of dynamic light scattering (DLS), which were based on the particle size analyzer instrument (Zetasizer Nano ZS, Malvern Instruments Ltd, UK). The concentration of each sample

solution was the same as 0.6 wt%. The intrinsic viscosity [η] of each sample in dilute polymer toluene solution was also obtained through the Ubbelohde viscometer at 70 °C.

3. Results and discussion

3.1. Reaction evolution

Generally, the polymer reactive processing is accompanied by the shear heating and reactive heating, which alter the temperature of sample. The shear heating becomes more evident as the system viscosity or rotational speed increases. Since the elevation of temperature can speedup the decomposition of the initiator (DCP) and change the kinetics of macromolecular reactions, the set temperature was lowered as the rotational speed increased in each processing course (Table 1) to compensate viscous heating. From Fig. 1, it can be observed that the evolutions of temperature are similar under all processing conditions. Therefore, the effect of temperature on the reactions can be ruled out. Since the torque depends on the molecular weight as well as the chain structure of polymer, it can be used to monitor the reaction evolution. In the case of RSC10 (10 rpm), the torque increased monotonously all the time and reached a plateau at around 14 min, which was the result of the coupling reactions of two macroradicals leading to an increase in the molecular weight and the degree of branching. The reaction was held for an extra 5 min, and no changes in the torque were observed, which revealed no further coupling and degradation reactions. Taking RSC10 as a reference, the torque in other cases increased first and then decreased with time. This non-monotonic behavior is attributed to the decrease of molecular weight since the temperature has already become a constant when the torque starts to decrease. This is probably induced by the degradation reaction under high rotational speed. It should be stressed that all the samples having the same formula and the temperatures are similar in all processing conditions. Therefore, any possible difference in molecular structure of products should be attributed to the difference in flow field.

3.2. Rheology

The small amplitude mechanical spectrometry of original PEB and all RSC products is shown in Fig. 2. The storage modulus G' of each product was much higher than that of the original PEB, indicating high molecular weight component created due to the coupling reaction. The slope of $\log G' \sim \log \omega$ at low frequency region becomes smaller than 2, the terminal behavior of linear PEB. This is similar to the behavior of LCB polypropylene made by reactive processing [10]. G' and the overall complex viscosity η^* descended with the processing rotational speed, which was attributed to the increasing degradation reactions as the rotational speed increases. The same inference could be given from the zero viscosity of each sample which was obtained from the creep test and is listed in Table 1. From the view of the reaction mechanism [3,4], it is the relative distance between two neighboring chains produced by β-scission that determines whether the degradation could happen. Actually, the nonlinear shear flow can strongly affect this distance, and the degradation will truly occur when the shear flow makes this distance larger than the capture radius. So in the present case, the nonlinear shear flow surely prevents the recombination of two scission parts and leads to the degradation in such reaction system.

However, neither the dynamic modulus nor the zero shear viscosity can clearly illustrate the difference in the chain structure of each sample due to the combined contributions of molecular weight and long chain branch. Fourier Transform Rheology (FTR) has been proved to be very sensitive to the existence of LCB. The nonlinear oscillatory shear is able to supply more detailed

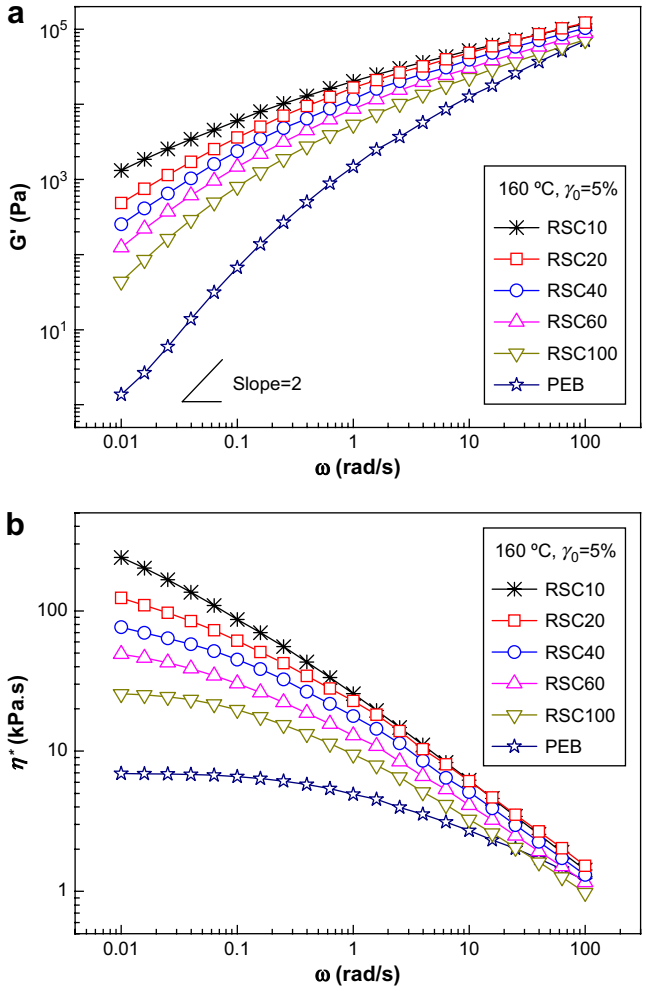

Fig. 2. Small amplitude mechanical spectrometry of the original PEB and all RSC products: (a) storage modulus; (b) complex viscosity (160 °C, $\gamma_0 = 5\%$).

information about the polymer architecture through analyzing the responses in the Fourier space. Usually, the third complex harmonic of stress (σ_3^*) was paid more attention and can be expressed as

$$\sigma_3^* = \sigma_3 \sin(3\omega t + \varphi_3) \quad (1)$$

where σ_3 and φ_3 denote the magnitude and phase of the third complex harmonic of stress, respectively. Correspondingly, σ_1 and φ_1 represent the magnitude and phase of the fundamental σ_1^*. Then the relative intensity of stress (σ_3/σ_1) and the phase shift ($\Phi_3 = \varphi_3 - 3\varphi_1$) can be chosen as parameters to characterize the nonlinear effect in the periodic stress curve [6–9].

It is shown that in the medium amplitudes' oscillatory shear (MAOS with γ_0 about 30–110%) [5], σ_3/σ_1 can be scaled with γ_0, where β is an indicator of the polymer topological structure and independent of the molecular weight, molecular weight distribution, and excitation frequency and temperature. The scaling exponent β remains constant "2" for linear polymer, but is lower than 2 for branched polymer. In the log–log plot of σ_3/σ_1 vs. γ_0, the slope (β) is nearly 2 for original PEB (Fig. 3(a)). The slopes for all RSC products fall in the range from 1.56 to 1.79 (the other three are not shown in the figure), which indicates the formation of LCB in the products. Furthermore, the scale β deviates from 2 more and more as the processing rotational speed decreases, which suggests the highest level of LCB in RSC10 sample. The change in LCB level under different processing conditions is ascribed to the difference in

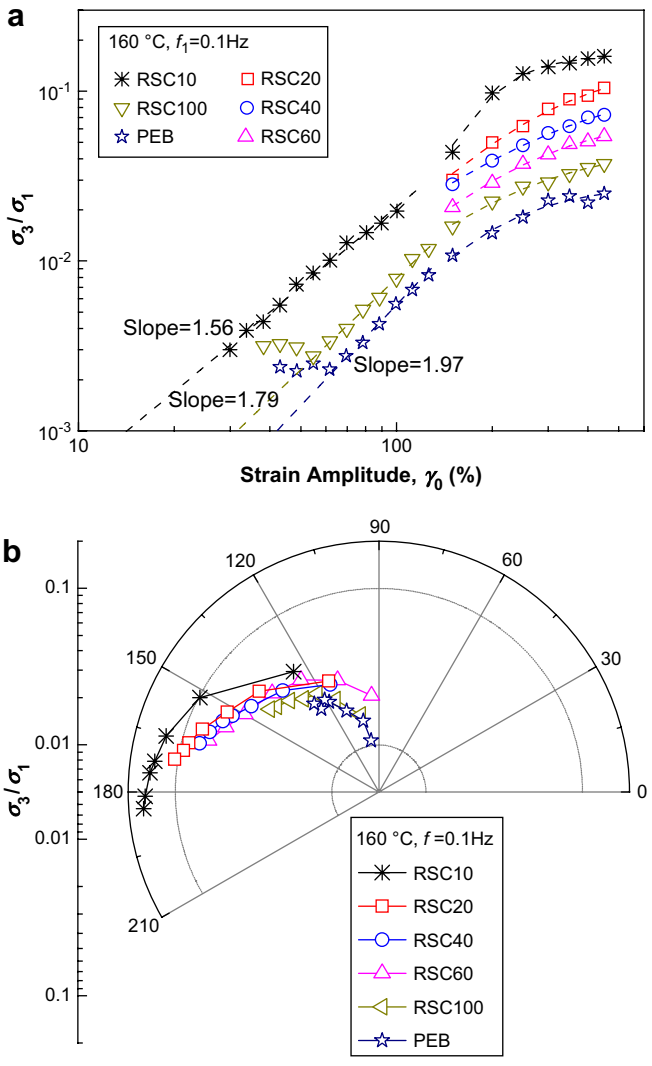

Fig. 3. The relative third stress intensity (σ_3/σ_1) of original PEB and RSC products as a function of (a) strain amplitude acquired by MAOS and LAOS and (b) the phase shift (Φ_3) acquired by LAOS (160°C, fundamental frequency $f_1 = 0.1$ Hz).

degradation probability under different flow fields. Decrease of β with the decrease of rotational speed during processing means stronger processing flow field can induce more degradation, which is consistent with the previous studies [3,4].

The difference in all samples can be further illustrated by the nonlinear rheological experiments with large oscillatory amplitudes from 150% to 450% (LAOS). As shown in Fig. 3(a), the relative stress intensities (σ_3/σ_1) for original PEB and all products were distinguished extremely over the entire range of studied strain amplitude. The higher the processing rotational speed was, the weaker the nonlinear rheological response of the product was. Because of the similar level of macromolecular radicals' concentration in each test with different rotational speed (due to the same concentration of peroxides in the samples), the number of LCB created through coupling should not be much different. Since it was already confirmed that the degrading behavior started to act on the LCB firstly [4], the various nonlinearities should be attributed to the statistically various arm lengths of LCB. For the largest processing rotational speed (RSC100), the nonlinearity curve becomes close to that of linear PEB, which suggested chains with almost linear structure and a small amount of LCB in RSC100 sample. The proposed reason should lie in the scission occurring so near the branching point that a certain amount of LCB degraded to be linear chains again in the case with 100 rpm. More distinct differences in the topological structure between products can be observed in the polar coordinate figure of σ_3/σ_1 vs. Φ_3 (Fig. 3(b)), where the nonlinearity notably increases with the radius of the half loop. According to the above, all the RSC products can be allocated into three groups, and it is easier to judge and differentiate how seriously the sample suffers from the degradation. These results show the possibility of controlling the level of LCB by the processing flow field.

3.3. DLS and intrinsic viscosity

The nonlinear architecture of LCB reduces the molecular dimension compared to the linear chain with the same molecular weight, which leads to the decrease in the viscosity. On the other hand, the viscosity of LCB increases much more than that of linear chain due to the entanglements of the LCB, which cannot relax only by the reptation. In this case, the dynamics of such molecules should involve the arm retraction mechanism. The method of dilute polymer solution can avoid the latter factor, which can be another way to characterize the polymer topological structure.

The hydrodynamic radius R_h is usually a measure of the molecular size, and related to the molecular weight M by

$$R_h = K_h \cdot M^{\alpha_h} \quad (2)$$

For linear polymer in good solvent, the exponent α_h is equal to 0.5 ~ 0.6. But for branching polymer with the same M as linear polymer, the scale becomes much smaller. The variation of exponent α_h can reflect the change of the polymer architecture. From the results of DLS experiments, the R_h distributions of all the samples were obtained and are displayed in Fig. 4. The intensity-weighted hydrodynamic radius $\overline{R}_h$ of all the samples is listed in Table 1. In Fig. 4, the curve of the product shifts to the position with smaller and smaller value of R_h as the processing rotational speed increases. In addition, another three points can be observed. Firstly, there's the difference between the curves of RSC10 and RSC20 but only in the larger R_h part. The disappearance of this part in RSC20 should be attributed to the tailoring on the created LCB through degradation when processing at 20 rpm. Secondly, the R_h distributions of RSC40 and RSC60 get narrower compared with those of RSC10 and RSC20. Finally, the double peaks in the curve of RSC100 probably indicate a certain amount of LCB returned to be linear chains again during the modification. Significant decrease of R_h was found as the processing rotational speed increases.

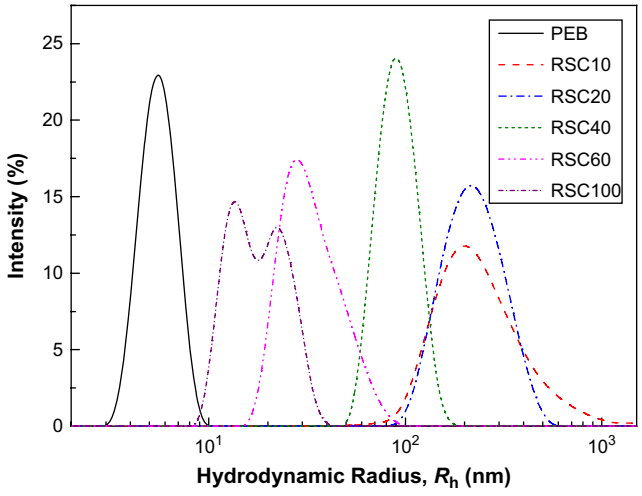

Fig. 4. Hydrodynamic radius distributions by DLS of the original PEB and all RSC products (70 °C, 0.6 wt% toluene solution).

On the basis of Zimm–Stockmayer analysis, the presence of LCB can cause the reduction of the hydrodynamic volume and one contraction factor ($g' = [\eta]_B/[\eta]_L$) is defined as the ratio of the intrinsic viscosity of branched polymer ($[\eta]_B$) to that of linear polymer ($[\eta]_L$) with the same molecular weight. The subscripts "B" and "L" denote the branched and linear polymers, respectively, also for the following part. So the intrinsic viscosity $[\eta]$ in dilute polymer solution was another indicator of chain structure, which depends on the molecular weight by the Mark–Houwink relation:

$$[\eta] = K_v \cdot M^{\alpha_v} \tag{3}$$

Then we can obtain the relationship between $[\eta]$ and R_h or η_0 as follows combining the zero shear viscosity–molecular weight relation, $\eta_0 = K_r \cdot M^{\alpha_r}$

$$[\eta] = K_1 \cdot R_h^{\alpha_1} \tag{4a}$$

$$[\eta] = K_2 \cdot \eta_0^{\alpha_2} \tag{4b}$$

where $K_1 = K_v/K_h^{\alpha_1}$, $K_2 = K_v/K_r^{\alpha_2}$, $\alpha_1 = \alpha_v/\alpha_h$ and $\alpha_2 = \alpha_v/\alpha_r$. α_r is taken as 3.5 for entangled flexible linear polymer PEB. Since $R_h \approx 0.75R_g$ for linear ethylene and α-olefin copolymer where R_g represents the radius of gyration [11], α_h can be considered to be the same as the exponent in R_g–M relationship. According to the data of PEB obtained in the solution of 1,2,4-trichlorobenzene (TCB) in Refs. [11,12], we can carry out some estimation here and choose 0.7 as the value for α_v and 0.59 for α_h. In this wise, $\alpha_{1,L} = 1.185$ and $\alpha_{2,L} = 0.2$, which are the slopes of the red dashed lines (passing through the point of original PEB) respectively in Fig. 5(a) and (b). Fig. 5(a) depicts the result in dilute polymer solution where there is only the effect of reduction of coil dimension, while Fig. 5(b) involves melt zero shear viscosity which truly reflects the effect of entanglements of LCB besides the former one. Clearly, there are similar results in both figures. All the reaction products deviate from those trend lines that denote nonlinear chain structures. Meanwhile, for the reaction products except RSC100, there's another scale between $[\eta]$ and R_h or η_0: $\alpha_{1,B} = 0.055$ or $\alpha_{2,B} = 0.065$, which are really much smaller than those for linear PEB and shown as the slopes of the solid trend lines. For linear chains, increase of molecular weight will cause the intrinsic viscosity increase a little bit faster than that of the hydrodynamic radius ($\alpha_v > \alpha_h$). For branched products, very small $\alpha_{1,B}$ means $\alpha_v \ll \alpha_h$. This suggests that the coil dimension is mainly affected by the molecular weight and has a relatively weak dependence on the formation of long chain branch, while intrinsic viscosity is strongly reduced with the formation of LCB. This is consistent with the common observation that the contraction factor defined by intrinsic viscosity (g') is smaller than that defined by the radius of gyration ($g = R_{g,B}^2/R_{g,L}^2$). This new scaling relationship implies that the number of branch points in these products is nearly the same. The reason why the point of RSC100 does not fall on the trend line with slope of $\alpha_{1,B}$ or $\alpha_{2,B}$ may be ascribed to the decrease of the LCB content due to the degeneracy of a certain amount of LCB to linear chains during the modification. All these results obtained in dilute polymer solution are in accordance with the nonlinear rheological properties demonstrated above.

3.4. Definition of the indicator of the polymer architecture

It has been illustrated above that rheology (linear and nonlinear oscillation), intrinsic viscosity and dynamic light scattering can show the difference in the chain structure of products. Moreover, quantitative evaluation of long chain branch can be obtained from certain combined analysis. Typically, the so-called g-factor or g'-factor is used to describe the effect of branches on the coil size or the

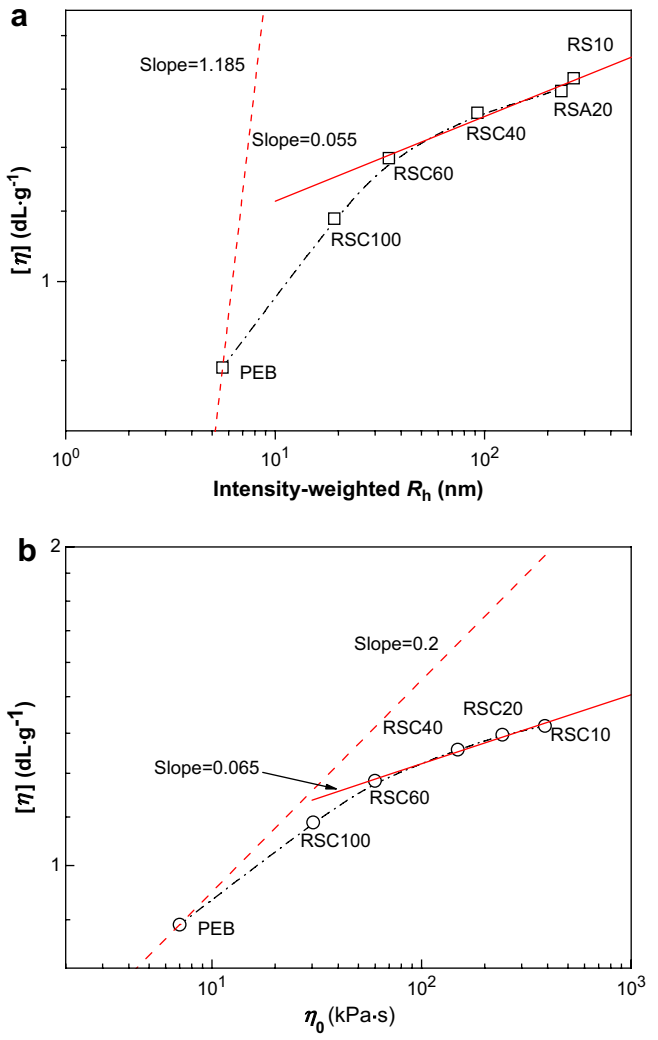

Fig. 5. The intrinsic viscosity $[\eta]$ at 70 °C of the original PEB and all RSC products as a function of (a) intensity-weighted hydrodynamic radius ($\overline{R}_h$) in 0.6 wt% toluene solution at 70 °C and (b) the melt zero viscosity (η_0) at 160 °C. (For interpretation of the references to colour in this figure, the reader is referred to the web version of this article.)

intrinsic viscosity. A long chain branching index (LCBI) is defined to quantify the level of LCB on the basis of viscosity enhancement from zero shear viscosity and intrinsic viscosity data [12]:

$$\mathrm{LCBI} = \frac{K_{2,L} \cdot \eta_0^{\alpha_{2,L}}}{[\eta]} - 1 \tag{5}$$

LCBI is zero for linear polymers without LCB while becomes larger for the LCB polymers due to the increasing effect of LCB on the rheology. It has been justified to be very powerful when applied on the essentially linear commercial [12] and the model ethylene/α-olefin copolymers [13]. The difficulty in the application of LCBI comes from the determination of parameters in Eq. (4b), which requires some linear polymers with different molecular weights and suitable solvent. In our cases, LCBI was calculated with $K_{2,L} = 1050 \times 10^{-2}$ [$\mathrm{kg^{-1.2}\,m^{3.2}\,s^{0.2}}$] (determined by $[\eta]$ and η_0 of PEB) and $\alpha_{2,L} = 0.2$, and is also listed in Table 1.

Considering the sensitivity of nonlinear rheological properties to the long chain branch, it is more convenient to define the level of LCB through melt rheological measurement. It is seen from Fig. 3(a) that nonlinearity σ_3/σ_1 increases with strain and approaches a constant value at high strain level. This behavior can be described by the following equation [6,9]

$$\frac{\sigma_3}{\sigma_1}(\gamma_0) = A\left(1 - \frac{1}{1 + (B\gamma_0)^C}\right) \tag{6}$$

Parameter A is the maximum intensity of σ_3/σ_1, the plateau at very large shear amplitudes. B is critical inverse strain amplitude when $\sigma_3/\sigma_1 = A/2$ and C is the power-law dependence for small strain amplitudes. All the experimental results of LAOS can be fitted by this equation and the corresponding fitting curve was already displayed by dashes in figures. Parameter A can be used to evaluate the level of LCB. However, the increase of the molecular weight can also lead to the increase of σ_3/σ_1. So the key point is how to exclude the effect caused by the increase of the molecular weight, or alternatively, we need to know the nonlinear response of a linear polymer with the same molecular weight as the branched one. This is the same idea as other definitions of LCB, such as LCBI.

It is known that linear polymers have a square scaling with strain amplitude under the medium amplitude oscillatory shear (MAOS) [5]. This behavior can also be predicted by some constitutive models, such as the coupled double-convection-reptation with chain stretching (cDCR-CS) model [14]

$$\frac{\sigma_3}{\sigma_1}(\gamma_0) = \frac{1}{8}\mathrm{De}^2\gamma_0^2 + O\left(\gamma_0^4\right) \tag{7}$$

where $\mathrm{De} = \omega\lambda$, is the Deborah number and depends only on the relaxation time λ of linear polymer chain. For branched chains, although it is shown that the scaling exponent decreases with increase of branch level, predictions from Pom–Pom model also show the square scaling for branched chains. This implies that the nonlinear response of linear polymers with different molecular weights can be by vertical shift of σ_3/σ_1. The shift curve is obtained by moving the σ_3/σ_1 curve of linear polymer (PEB here) vertically with a shifting factor a_I (Fig. 6) to be superposed with curve of branched polymer in the low strain limit of MAOS region. The branched level can be defined as

$$D_{\mathrm{LCB}} = \frac{A_B}{A_L \cdot a_I} - 1 \tag{8}$$

where the variable A is the coefficient in Eq. (6) and a_I is the shifting factor. The values of revised D_{LCB} for all samples were obtained and are listed with a_I in Table 1. The indicator of D_{LCB} only comes from the nonlinear rheological properties of polymer melt. Now we extend D_{LCB} with LCBI and plot them in Fig. 7, where it can be seen that one good proportional relationship can be established between these two parameters for all samples. That is to say, this relationship is always valid no matter which the topological structure of the sample is, so this plot shows a map and defines a way to quantify the level of LCB only by FTR.

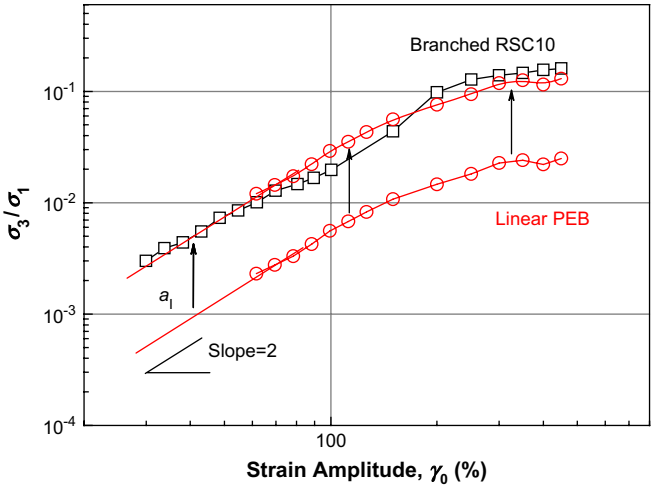

Fig. 6. The sketch of moving σ_3/σ_1 curve of PEB by the shifting factor a_I.

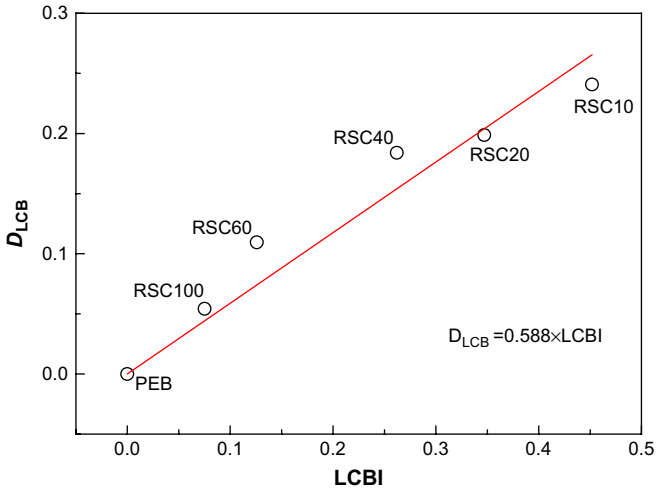

Fig. 7. The relationship between D_{LCB} and LCBI for all the samples.

4. Conclusion

With the compensation of temperature, the strength of complex shear flow on the architecture of the product polymer in the torque rheometer was investigated. The results gained from DSL and FTR indicated that the degradation still started on LCB and the length of LCB decreased with the rotational speed. In addition, D_A is defined as the indicators of LCB which is nearly proportional to the long chain branching index (LCBI). Thus a map to quantify LCB level only by Fourier Transform Rheology (FTR) is established. Although the rotational speed cannot represent the complex flow field exactly, all the characterizations can give the significant instruction to tailor the polymer architecture more or less. We only have one adjustable window of the topological structure and content of LCB (between RSC10 and RSC100) here through altering the processing flow field, but it can be imaged that there could be no LCB and the length of linear chain is even shorter than that of original PEB if stronger flow field could be applied such as in twin screw extruder.

Acknowledgements

The authors thank financial support for this work from the *National Natural Science Foundation of China* (No. 50390095 and No. 20574045).

References

[1] Vega JF, Muñoz EA, Santamaría A, Muñoz ME, Lafuente P. Macromolecules 1996;29(3):960–5.
[2] Liu MG, Yu W, Zhou CX. J Appl Polym Sci 2006;100(1):839–42.
[3] Liu JY, Yu W, Zhou CX. Polymer 2006;47(20):7051–9.
[4] Liu JY, Yu W, Zhou CX. Polymer 2008;49(1):268–77.
[5] Hyun K, Baik ES, Kim SH, Ahn KH, Lee SJ, Sugimoto M, et al. J Rheol 2007;51(6):1319–42.
[6] Neidhöfer T, Wilhelm M. J Rheol 2003;47(6):1351–71.
[7] Neidhöfer T, Sioula S, Hadjichristidis N, Wilhelm M. Macromol Rapid Commun 2004;25(22):1921–6.
[8] Schlatter G, Fleury G, Muller R. Macromolecules 2005;38(15):6492–503.
[9] Vittorias I, Parkinson M, Klimke K, Debbaut B, Wilhelm M. Rheol Acta 2007;46(3):321–40.
[10] Tian JH, Yu W, Zhou CX. Polymer 2006;47(23):7962–9.
[11] Sun T, Brant P, Chance RR, Graessley WW. Macromolecules 2001;34(19):6812–20.
[12] Shroff RN, Mavridis H. Macromolecules 1999;32(25):8454–64.
[13] César AGF, David JL, Christopher GR, Olivier G. Eur Polym J 2008;44(2):376–91.
[14] Marrucci G, Ianniruberto G. Philos Trans R Soc London Ser A 2003;361:677–88.